nature communications

Article

https://doi.org/10.1038/s41467-025-59968-9

NNMT/1-MNA protects against hepatic ischemia-reperfusion injury through the AKT/FOXO1/ANGPT2/JNK axis

Received: 24 October 2024

Accepted: 5 May 2025

Published online: 22 May 2025

Check for updates

Bing Yin[1,2,11], Baolin Qian[1,2,11], Hongjun Yu[1,2,11], Shanjia Ke[1,2,11], Zihao Li[1,2], Yongliang Hua[2,3], Shounan Lu[1,2], Chaoqun Wang[1,2], Mengxin Li[4], Sixun Guo[5], Zhongyu Li[1,2], Yongzhi Zhou[1,2], Zhanzhi Meng[1,2], Xinglong Li[1,2], Yanan Xu[2,6], Zhigang Feng[2,7], Miaoyu Bai[1,2], Yao Fu[8], Wei Tang[9,10], Shangyu Hong[1,4] ✉ & Yong Ma[1,2] ✉

Hepatic ischemia–reperfusion injury (HIRI) occurs during liver surgery, contributing to postoperative complications such as liver failure, prolonged hospital stays, and increased morbidity and mortality rates. Yet, the mechanism underlying HIRI remains unclear. Nicotinamide N-methyltransferase (NNMT) facilitates the conversion of nicotinamide into N^1-methylnicotinamide (1-MNA) and plays crucial roles in various pathophysiological processes. In this study, we find a decrease in hepatic NNMT expression and serum 1-MNA levels during HIRI. Both NNMT overexpression and exogenous 1-MNA treatment alleviate HIRI in male mice HIRI models and primary hepatocytes H/R models. Mechanistically, NNMT/1-MNA plays key roles in inflammation, apoptosis, and vascular injury during HIRI through the AKT/FOXO1/ANGPT2/JNK axis. Hepatic-specific depletion of NNMT leads to increased ANGPT2 expression and exacerbates HIRI, effects that can be mitigated by ANGPT2 knockdown. Our findings suggest that NNMT/1-MNA/ANGPT2 may regulate HIRI via the JNK signaling pathway. In summary, we present the function of NNMT and its underlying mechanism in liver injury, providing potential new therapeutical strategies for addressing HIRI.

Hepatic ischemia-reperfusion injury (HIRI) refers to the damage inflicted on liver tissue when blood supply is temporarily interrupted (ischemia) and subsequently restored (reperfusion). HIRI holds paramount importance in various surgical contexts such as liver transplantation, liver resection, or trauma-related events[1,2]. During ischemia, the liver tissue undergoes oxygen and nutrient deprivation, resulting in cellular dysfunction and metabolic derangements[3]. Upon reperfusion, the sudden reintroduction of oxygen-rich blood triggers

[1]Department of Minimally Invasive Hepatic Surgery, The First Affiliated Hospital of Harbin Medical University, Harbin, China. [2]Key Laboratory of Hepatosplenic Surgery, Ministry of Education, Harbin, China. [3]Department of Pediatric Surgery, the Sixth Affiliated Hospital of Harbin Medical University, Harbin, China. [4]State Key Laboratory of Genetic Engineering, School of Life Sciences, Fudan University, Shanghai, China. [5]Department of Pharmacy, The First affiliated Hospital of Harbin Medical University, Harbin, China. [6]Department of Hepatopancreatobiliary Surgery, Affiliated Hangzhou First People's Hospital, Zhejiang University School of Medicine, Hangzhou, China. [7]The First Department of General Surgery, The Affiliated Hospital of Inner Mongolia Minzu University, Tongliao, China. [8]Department of Ultrasound, The First Affiliated Hospital of Harbin Medical University, Harbin, China. [9]International Health Care Center, National Center for Global Health and Medicine, Tokyo, Japan. [10]Hepato-Biliary-Pancreatic Surgery Division, Department of Surgery, The University of Tokyo Hospital, Tokyo, Japan. [11]These authors contributed equally: Bing Yin, Baolin Qian, Hongjun Yu, Shanjia Ke. ✉e-mail: shangyu_hong@fudan.edu.cn; mayong@ems.hrbmu.edu.cn

https://doi.org/10.1038/s41467-025-59968-9

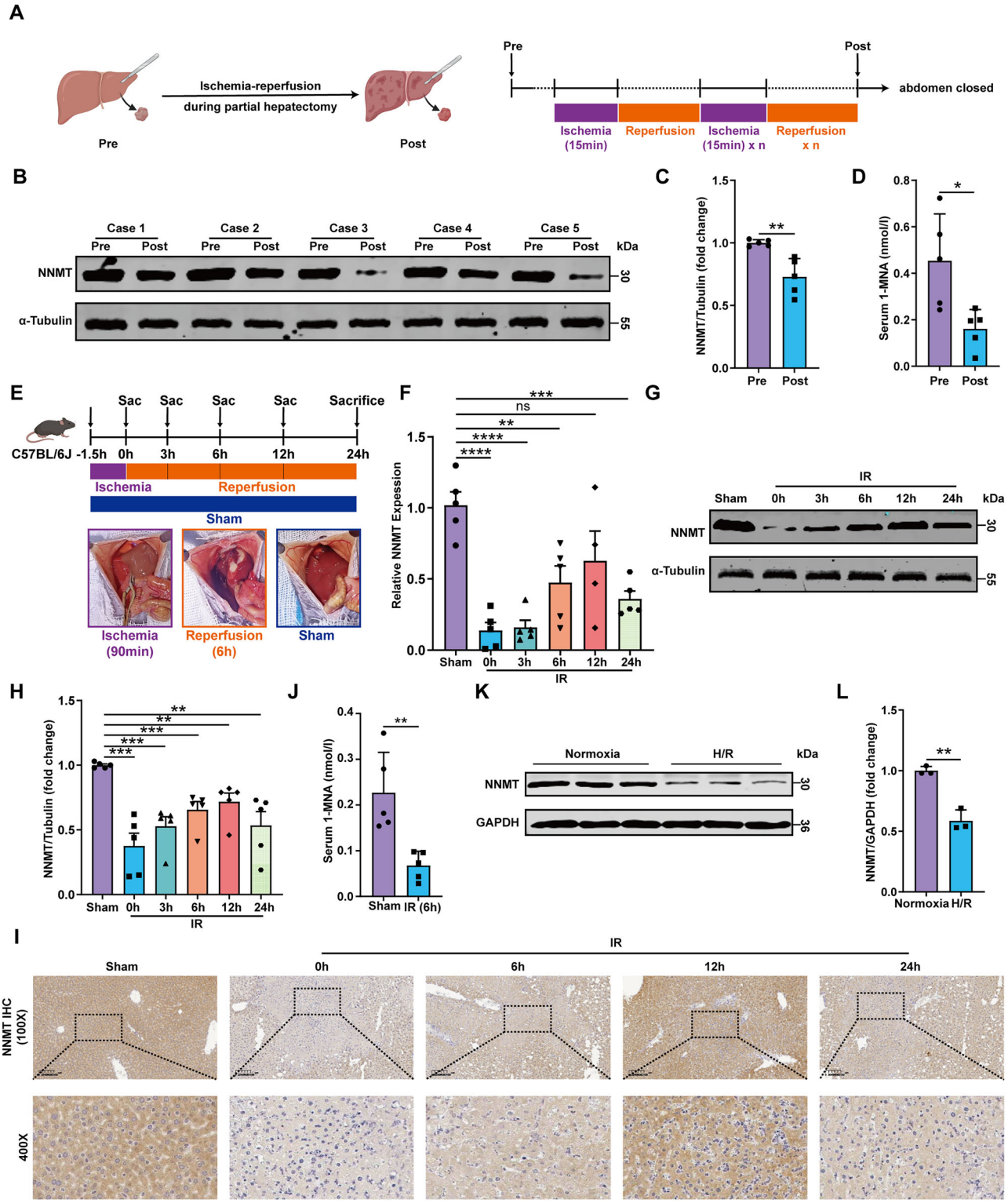

Fig. 1 | The expression of NNMT and the levels of 1-MNA decreased after HIRI. **A** The clinical liver specimens obtained from patients undergoing partial hepatectomy. **B**, **C** The expression level of NNMT in clinical samples ($n = 5$, $P = 0.003425$). **D** The serum concentration of 1-MNA in patients with partial hepatectomy. **E** Illustration of the experimental procedures ($n = 5$, $P = 0.01708$). **F**–**H** The mRNA and protein levels of NNMT in a mouse HIRI model (**F**: $n = 5$, $P = 0.000044$, 0.000043, 0.006934, 0.109756, 0.00032; **H**: $n = 5$. $P = 0.000232$, 0.000201, 0.00061, 0.002913, 0.002433). **I** The immunohistochemical staining of NNMT in the livers (scale bar: 100 μm). **J** The serum concentration of 1-MNA in a mouse HIRI model ($n = 5$, $P = 0.00521$). **K**, **L** The expression level of NNMT in a mouse primary hepatocyte model of H/R ($n = 3$, $P = 0.001734$). The results are expressed as mean ± SD. Three biologically independent experiments. Source data are provided as a Source data file. Figure 1A,E were created in BioRender. Bing, Y. (2025) https://BioRender.com/vesbjfg. H/R Hypoxia and reoxygenation, IHC immunohistochemistry, IR ischemia reperfusion, 1-MNA N[1]-methylnicotinamide, NNMT Nicotinamide N-methyltransferase, IHC immunohistochemistry, Pre preoperative, Post postoperative.

https://doi.org/10.1038/s41467-025-59968-9

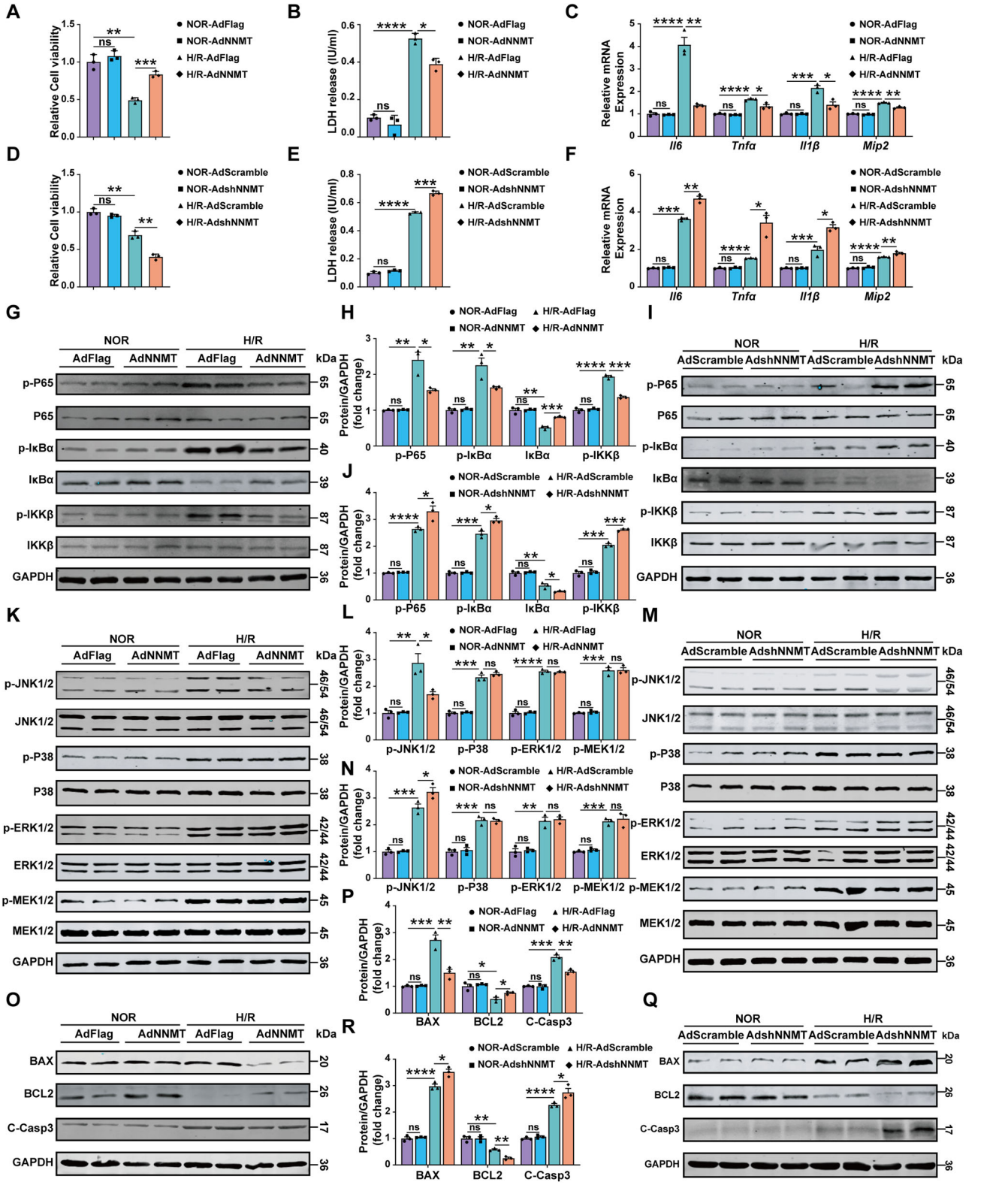

a cascade of inflammatory responses and oxidative stress[4], leading to the production of pro-inflammatory cytokines and chemokines, activation of the NF-κB and MAPK signaling pathways, initiation of the intracellular inflammatory cascade, stimulation of the adaptive immune response, and ultimately, aggravation of hepatocyte necrosis and apoptosis[5]. Effectively mitigating the adverse effects of HIRI remains a clinical challenge, and the precise underlying mechanism of this phenomenon is yet to be fully understood.

Nicotinamide N-methyltransferase (NNMT) catalyzes the conversion of nicotinamide (NAM) to N^1-methylnicotinamide (1-MNA) and plays a crucial role in regulating various hepatic pathophysiological processes[6–10]. Moreover, treatment with 1-MNA reduces liver transaminases, ameliorates hepatic injury, and suppresses the secretion of inflammatory mediators[11]. Building upon our prior RNA-seq data pertaining to HIRI[12–14], which showed that NNMT is one of the significantly changed genes, we aim to elucidate the

Fig. 2 | NNMT protected against H/R-induced inflammation and apoptosis. **A** The CCK-8 assay in primary hepatocytes indicating cell viability ($n = 3$, $P = 0.001145$, 0.000417). **B** The LDH levels indicating cell death ($n = 3$, $P = 0.000022$, 0.005097). **C** The mRNA levels of IL-6, TNF-α and MIP-2 in primary hepatocytes ($n = 3$, $P = 0.000794$, 0.001265, 0.000059, 0.022793, 0.000491, 0.011172, 0.000029, 0.004128). **D**–**F** The cell viability, LDH levels, and mRNA expression of inflammatory cytokines in primary hepatocytes infected with *Nnmt* knockdown virus (**D**: $n = 3$, $P = 0.001539$, 0.001623; **E**: $n = 3$, $P = 0.0000004$, 0.000142; **F**: $n = 3$, $P = 0.000001$, 0.001327, 0.000022, 0.008395, 0.005692, 0.006005, 0.000007, 0.016065). **G**–**J** The NF-κB signaling pathway in primary hepatocytes (**H**: $n = 3$, $P = 0.002815$, 0.017879, 0.003711, 0.038824, 0.001359, 0.000751, 0.000044, 0.000163; **J**: $n = 3$, $P = 0.000008$, 0.033984, 0.000105, 0.012657, 0.003946, 0.028127, 0.000152, 0.000561). **K**–**N** The MAPKs signaling pathway in primary hepatocytes (**L**: $n = 3$, $P = 0.006622$, 0.031933, 0.00018, 0.305339, 0.000038, 0.520874, 0.0001, 0.917025; **N**: $n = 3$, $P = 0.000368$, 0.046641, 0.000543, 0.810961, 0.002784, 0.717269, 0.000125, 0.619467). **O**–**R** The apoptosis signaling pathway in primary hepatocytes (**P**: $n = 3$, $P = 0.000822$, 0.005915, 0.010552, 0.032551, 0.000129, 0.00401; **R**: $n = 3$, $P = 0.00005$, 0.015607, 0.004799, 0.002158, 0.000039, 0.045242). Data are showed as mean ± SD. Three biologically independent experiments. Source data are provided as a Source data file. AdFlag Gene overexpression negative control adenovirus, AdNNMT NNMT overexpression adenovirus, AdScramble Gene knockdown negative control adenovirus, AdshNNMT NNMT knockdown adenovirus, BAX BCL2 associated X protein, BCL2 B cell lymphoma 2, C-Casp3 Cleaved caspase-3, H/R Hypoxia and reoxygenation, *Il1β* Interleukin 1beta, *Il6* Interleukin 6, LDH Lactate dehydrogenase, *Mip2* Macrophage Inflammatory Protein 2, NOR Normoxia, *Tnfα* Tumor necrosis factor α.

precise mechanism underlying the role of NNMT/1-MNA in this process.

Angiopoietins (ANGPTs) comprise a family of cytokines crucial for vascular homeostasis[15]. Among ANGPTs, ANGPT2 expression is upregulated during cardiac ischemia–reperfusion injury, exacerbating myocardial hypoxia and inflammation. Inhibition of ANGPT2 has been shown to provide cardiac protection in experimental models[16,17]. Previous studies have demonstrated the specificity of ANGPT2 to vascular endothelial cells; however, it is noteworthy that ANGPT2 exhibits varying degrees of expression and regulation in tumor cells[18], T cells[19], and hepatocytes[20]. In this study, we aim to clarify the functional changes of ANGPT2 in hepatocytes and its overall functional changes in vivo regulation of HIRI.

In this study, we observed a decrease in NNMT expression and 1-MNA levels following HIRI. Our data demonstrated the protective effects of NNMT/1-MNA against HIRI. NNMT/1-MNA suppressed ANGPT2 expression, through the AKT/FOXO1 pathway, thereby mitigating inflammation, apoptosis, and vascular injury, NNMT/1-MNA/ANGPT2 may regulate HIRI via the JNK signaling pathway.

Results

HIRI decreased hepatic NNMT expression and 1-MNA contents

To explore the molecular mechanisms underlying liver injury in the context of HIRI and identify potential drug targets to meet clinical demands, we collected liver tissues and serum from patients undergoing partial hepatectomy for benign diseases before and after liver ischemia and reperfusion (Fig. 1A). After screening for key players whose expression responds to repeated ischemia-reperfusion in these samples, we found a significant reduction in NNMT expression upon HIRI (Fig. 1B, C). Concurrently, there was a significant decrease in serum 1-MNA content following HIRI (Fig. 1D). We established a mouse model of HIRI by subjecting to 90 min of partial hepatic ischemia followed by reperfusion (Fig. 1E). We observed a decrease in both the mRNA and protein levels of NNMT after HIRI compared with the sham group (Fig. 1F–H). Immunohistochemical results confirmed the downregulated *Nnmt* expression in mouse hepatocytes (Fig. 1I). Consistently, the serum 1-MNA content exhibited a significant decrease after the process of ischemia-reperfusion (Fig. 1J). Moreover, we isolated mouse primary hepatocytes and established an in vitro hypoxia and reoxygenation (H/R) cell model. Western blot results showed that there is less NNMT protein in hepatocytes experienced H/R compared to the normoxia group (Fig. 1K, L). These findings indicate a reduction in NNMT expression and 1-MNA content following HIRI, suggesting NNMT might play roles during this process.

NNMT alleviated HIRI-induced inflammation and apoptosis in vitro and in vivo

To investigate the role of NNMT in HIRI, we infected primary hepatocytes with adenovirus for *Nnmt* overexpression and knockdown, followed by a cell H/R process. The *Nnmt* overexpression and knockdown efficiency were confirmed by Western blot (Fig. S1A–D). *Nnmt* overexpression did not do much to hepatocytes in normoxia but significantly improved cell viability and inhibited cell death and inflammation in primary hepatocytes (Fig. 2A–C) in the context of H/R, as evidenced by the CCK-8 assay (cell viability), LDH assay (cell death) and the expression level of inflammation-related genes. Conversely, *Nnmt* knockdown significantly suppressed cell viability and increased cell death and inflammation (Fig. 2D–F). Next, we investigated classic inflammatory and apoptotic signaling pathways, observing a robust activation of NF-κB signaling pathway following H/R stimulation in primary hepatocytes (Fig. 2G–J). *Nnmt* overexpression effectively suppressed the H/R-induced NF-κB signaling pathway, while *Nnmt* knockdown significantly enhanced NF-κB signaling in the cells subjected to H/R (Fig. 2G–J). *Nnmt* overexpression led to a significant decrease in JNK phosphorylation, whereas *Nnmt* knockdown resulted in increased JNK phosphorylation in the context of H/R (Fig. 2K–N). NNMT manipulation did not alter the phosphorylation level of other targets within the MAPKs signaling pathway, such as P38, ERK1/2, and MEK1/2 (Fig. 2K–N). In addition, H/R treatment induced cell apoptosis, indicated by a significant increase of the pro-apoptotic proteins BAX and cleaved caspase-3, and a decrease in anti-apoptotic protein BCL2 (Fig. 2O–R). *Nnmt* overexpression inhibited H/R-induced cell apoptosis, while *Nnmt* knockdown exacerbated apoptosis in hepatocytes (Fig. 2O–R). Furthermore, like *Nnmt* knockdown, pretreatment with the NNMT-specific inhibitor JBSNF-000088 aggravated the H/R-induced cell inflammation and apoptosis (Fig. S2A–H).

Next, we investigated the roles of NNMT in vivo by tail vein injection of an adenovirus overexpressing *Nnmt* (Fig. S3A) or administration of JBSNF-000088 (Fig. S4A) in the HIRI mouse model. Overexpression of *Nnmt* alleviated ischemia-reperfusion-induced-liver injury and inflammation following HIRI, indicated by serum levels of ALT, AST and inflammatory factors, and the expression of inflammation-related genes in the liver (Fig. S3B–D), whereas inhibition of NNMT aggravated liver injury and inflammation (Fig. S4B–D). H&E staining results indicated that overexpression of *Nnmt* reduced the size of injured and necrotic areas in the liver (Fig. S3E, F), while inhibition of NNMT had the opposite effect (Fig. S4E, F). Immunofluorescence staining of liver sections revealed a reduction in the number of Ly6G- or CD11b-positive cells following *Nnmt* overexpression, again, suggesting an attenuated inflammatory response (Fig. S3G, H), while inhibition of NNMT increased the numbers of these cells (Fig. S4G, H). Levels of Ly6G mRNA were significantly reduced in the liver of NNMT overexpression mice than control mice after HIRI (Fig. S5A, B). Western blot analysis showed that overexpression of *Nnmt* suppressed ischemia-reperfusion-induced activation of NF-κB and JNK signaling pathways (Fig. S3I–L), while inhibition of NNMT resulted in stronger NF-κB and JNK signaling pathways (Fig. S4I–L). In addition, *Nnmt* overexpression alleviated cell apoptosis in the context of HIRI, indicated

https://doi.org/10.1038/s41467-025-59968-9

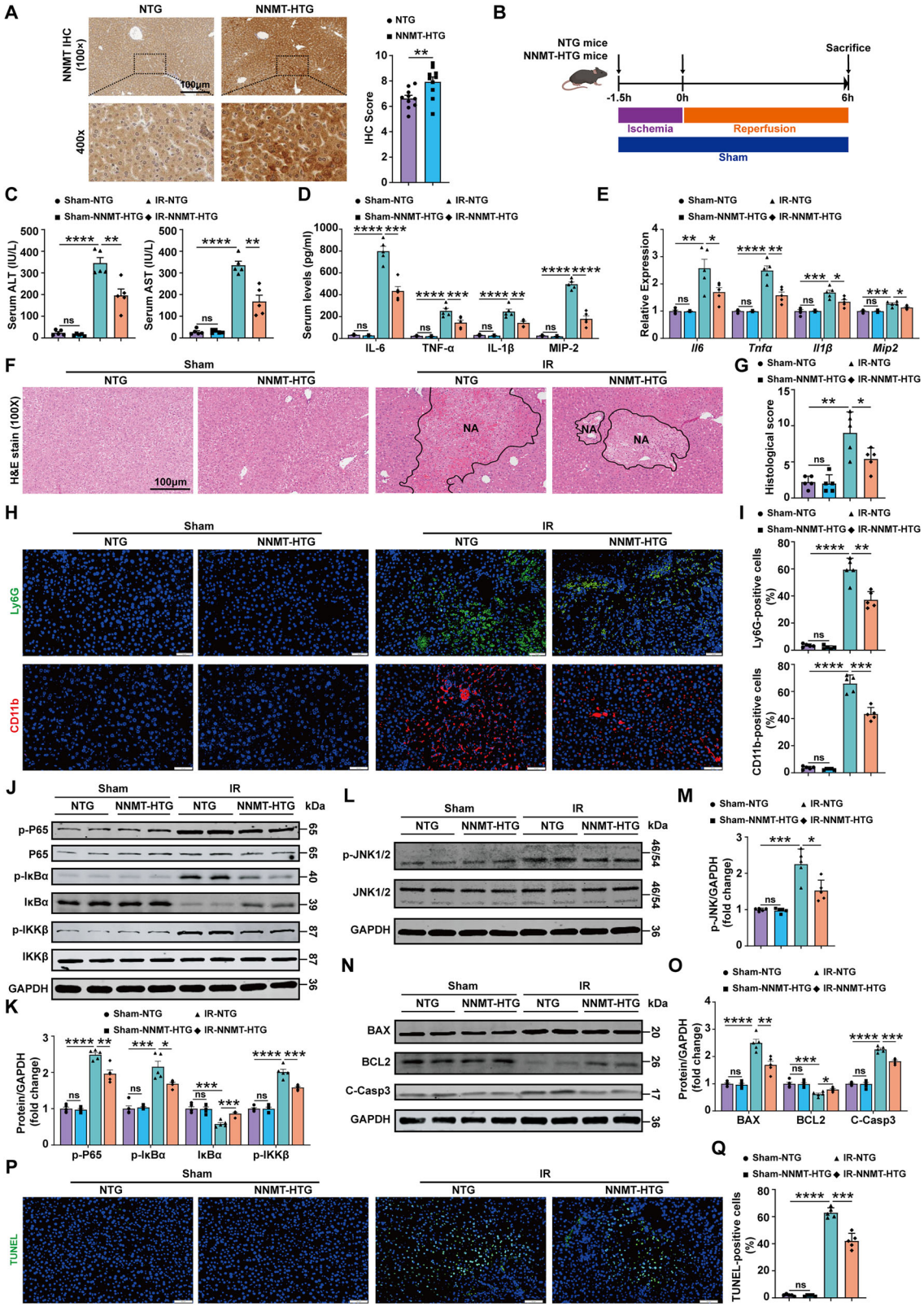

by a significant decrease of BAX and cleaved caspase-3, and an increase in anti-apoptotic protein BCL2, and fewer TUNEL-positive cells in mouse liver (Fig. S3M-P). Conversely, inhibition of NNMT aggravated cell apoptosis (Fig. S4M–P).

These findings suggest that NNMT plays a protective role against inflammation and apoptosis in the context of HIRI, both in vitro and in vivo.

1-MNA alleviated HIRI-induced inflammation and apoptosis in vitro and in vivo

1-MNA, the product of NNMT, plays crucial roles in various diseases[7,11]. We sought to determine whether 1-MNA could play a protective role against HIRI. In vitro, pretreatment with 1-MNA did not alter the biological activity of primary hepatocytes under normoxic conditions but significantly enhanced cell viability and

Fig. 3 | Hepatocyte-specific *Nnmt* overexpression protected against liver injury, inflammation and apoptosis induced by ischemia-reperfusion. **A** Immunohistochemical staining of NNMT in the livers (scale bar: 100 μm) ($n = 10$, $P = 0.009861$). **B** Illustration of the experimental procedures. **C** The serum transaminase levels in mice ($n = 5$, $P = 0.000001$, 0.004772, 0.0000002, 0.001296). **D** The serum levels of inflammation cytokines in mice ($n = 5$, $P = 0.0000001$, 0.000317, 0.000013, 0.012379, 0.000018, 0.006009, 0.00000001, 0.000015). **E** The mRNA level of inflammation cytokines in the liver ($n = 5$, $P = 0.001521$, 0.044657, 0.000022, 0.00223, 0.000202, 0.020573, 0.000412, 0.0236). **F**, **G** The extent of liver injury and necrosis following HIRI (scale bar: 100 μm) ($n = 5$, $P = 0.001036$, 0.039969). **H**, **I** The population of Ly6G- and CD11b-positive cells in the liver (scale bar: 50 μm) ($n = 5$, $P = 0.0000005$, 0.001377, 0.00000002, 0.000236). **J**, **K** The NF-κB signaling pathway in the liver ($n = 5$, $P = 0.00000004$, 0.002119, 0.000147, 0.018743, 0.000274, 0.000422, 0.000002, 0.000755). **L**, **M** The JNK signaling pathway in the liver ($n = 5$, $P = 0.000149$, 0.012319). **N**, **O** The apoptosis signaling pathway in the liver ($n = 5$, $P = 0.000005$, 0.002495, 0.000592, 0.01251, 0.0000000096, 0.000143). **P**, **Q** The population of TUNEL-positive cells in the liver (scale bar: 50 μm) ($n = 5$, $P = 0.0000000004$). Data are presented as mean ± SD. Three biologically independent experiments. Source data are provided as a Source data file. Figure 3B was created in BioRender. Bing, Y. (2025) https://BioRender.com/vesbjfg. ALT Alann amino transferase, AST Aspartate amino transferase, BAX BCL2 associated X protein, BCL2 B cell lymphoma 2, C-Casp3 Cleaved caspase-3, CD11b Integrin subunit alpha M, H&E Hematoxylin & eosin, IHC Immunohistochemistry, *Il1β*/IL-1β Interleukin 1beta, *Il6*/IL-6 Interleukin 6, IR Ischemia reperfusion, LDH Lactate dehydrogenase, Ly6G Lymphocyte antigen 6 complex locus G, *Mip2*/MIP-2 Macrophage Inflammatory Protein 2, NNMT-HTG NNMT hepatocyte transgene mouse, NTG Non-transgenic mouse, *Tnfα*/TNF-α tumor necrosis factor α, TUNEL Terminal dUTP Nick-End Labeling.

suppressed cell death and inflammation after H/R (Fig. S6A–C). In vivo, intraperitoneal injection of 1-MNA in a HIRI model significantly alleviated liver injury, suppressed inflammation, and reduced the size of injured and necrotic areas in the liver (Fig. S7A–I). 1-MNA suppressed the activation of the NF-κB, JNK and apoptotic signaling pathways, exerting a significant inhibitory effect on inflammation and apoptosis in vitro (Fig. S6D–I) and in vivo (Fig. S7J–O). Injection of 1-MNA in a HIRI model resulted in significantly fewer TUNEL-positive cells in mouse liver (Fig. S7P, Q). In summary, these findings demonstrate that 1-MNA protect against HIRI both in vitro and in vivo.

Hepatocyte-specific *Nnmt* transgenic mice exhibit reduced liver injury, inflammation, and apoptosis in the context of HIRI

Next, we generated hepatocyte-specific *Nnmt* transgenic (NNMT-HTG) mice, and validated *Nnmt* overexpression in mouse livers by western blot (Fig. S8A, B). Immunohistochemical results demonstrated the *Nnmt* overexpression in mouse hepatocytes (Fig. 3A). The HIRI model was induced in these NNMT-HTG mice and non-transgenic (NTG) control mice (Fig. 3B). Consistent with the results from mice injected with *Nnmt* overexpression virus, in NNMT-HTG mice, *Nnmt* overexpression resulted in a reduction in ischemia-reperfusion-induced liver injury and inflammation (Fig. 3C–G). The livers from mice with *Nnmt* overexpression have significantly fewer Ly6G- and CD11b-positive cells and suppressed NF-κB and JNK signaling pathways compared to the NTG group (Fig. 3H–M). Level of Ly6G mRNA was significant reduced in the liver of NNMT-HTG mice than NTG mice after HIRI (Fig. S9A). In addition, *Nnmt* overexpression alleviated cell apoptosis in the context of HIRI (Fig. 3N–Q). Overall, our results demonstrated that hepatic NNMT can mitigate liver injury and suppress inflammation and apoptosis, providing protection against the negative impacts of HIRI.

Hepatocyte-specific *Nnmt* knockout exacerbated liver injury, inflammation, and apoptosis in the context of HIRI

Next, we employed previously generated hepatocyte-specific *Nnmt* knockout mice ($NNMT^{\Delta Hep}$)[9] to verify the function of NNMT in the context of HIRI (Fig. S10A). *Nnmt* knockout mice have non-detectable NNMT expression in their liver (Fig. S10B). Immunohistochemical results further confirmed the depletion of *Nnmt* in mouse hepatocytes (Fig. 4A). The HIRI model was induced in $NNMT^{\triangle Hep}$ mice and the flox/flox control mice (Fig. 4B). *Nnmt* knockout exacerbated ischemia-reperfusion-induced liver injury and inflammation (Fig. 4C–G). The $NNMT^{\Delta Hep}$ mice had more Ly6G- and CD11b-positive cells and stronger NF-κB and JNK signaling in their livers (Fig. 4H–M). Levels of Ly6G mRNA were significantly increased in the liver of $NNMT^{\Delta Hep}$ mice than flox/flox mice after HIRI (Fig. S9B). In line with results from NNMT inhibitor treated mice, *Nnmt* knockout aggravated cell apoptosis (Fig. 4N–Q). In summary, our results revealed that depletion of hepatic *Nnmt* led to worse liver injury, exacerbated hepatic inflammation and apoptosis in the context of HIRI.

NNMT/1-MNA regulated the AKT/FOXO1/ANGPT2 axis and increases ANGPT2 expression

To further explore the mechanism underlying the protective roles of NNMT/1-MNA in HIRI, RNA sequencing of primary hepatocytes and liver tissues was conducted to identify the downstream targets of NNMT and 1-MNA (Fig. 5A). RNA-seq results revealed that the overexpression of *Nnmt* in primary hepatocytes during H/R led to 68 downregulated genes and 17 upregulated genes compared to the control group (Fig. 5B, D). Treatment with 1-MNA in mice downregulated a total of 175 genes in the liver, while 132 genes were upregulated (Fig. 5C, E). We found three genes, angiopoietin 2 (ANGPT2), aryl hydrocarbon receptor nuclear translocator-like 2 (ARNTL2), and cAMP responsive element binding protein 5 (CREB5) were downregulated in response to both *Nnmt* overexpression and 1-MNA treatment (Fig. 5F). However, the mRNA levels of CREB5 (Fig. 5G) and the protein levels of ARNTL2 (Figure S11) were not significantly regulated by NNMT/1-MNA. Only the reduction of ANGPT2 was confirmed both in mRNA- and protein-level by RT-qPCR and western blot (Fig. 5G–I). Previous studies[16,17] have shown that ANGPT2 plays an important role in the processes of ischemia and hypoxia after myocardial infarction, suggesting that ANGPT2 might be the key factor downstream of NNMT/1-MNA, and play important roles in HIRI. There's no overlapped gene that was upregulated in both cases. KEGG enrichment analysis suggested that differentially expressed genes were significantly enriched in the PI3K/AKT signaling pathway after *Nnmt* overexpression (Fig. 5J). Previous reports showed that FOXO1, a well-known downstream target of AKT, regulates the expression of ANGPT2[21,22]. Thus, we hypothesized that NNMT/1-MNA might inhibit ANGPT2 expression through the AKT/FOXO1/ANGPT2 axis. Consistent with this hypothesis, *Nnmt* overexpression or treatment with 1-MNA in primary hepatocytes increased AKT phosphorylation and decreased FOXO1 expression (Fig. 5K, L). In this context, FOXO1 overexpression resulted in an increase in ANGPT2 expression (Fig. 5M, N). On the other hand, we treated primary hepatocytes with the PI3K/AKT specific inhibitor PI3K/AKT-IN-1 and found that the inhibitory effect of NNMT/1-MNA on FOXO1 and ANGPT2 was partially reduced (Fig. 5O–R).

In conclusion, our findings suggest that NNMT/1-MNA exerts inhibitory effects on ANGPT2 expression via the AKT/FOXO1 axis during HIRI.

ANGPT2 aggravated HIRI-induced inflammation, apoptosis, and vascular injury

Next, we investigated whether ANGPT2 play roles in HIRI. First, we observed that the expression of ANGPT2 was significantly increased following HIRI in patients, mouse, and primary hepatocytes (Fig. S12A–C). Second, we generated ANGPT2 overexpression and

https://doi.org/10.1038/s41467-025-59968-9

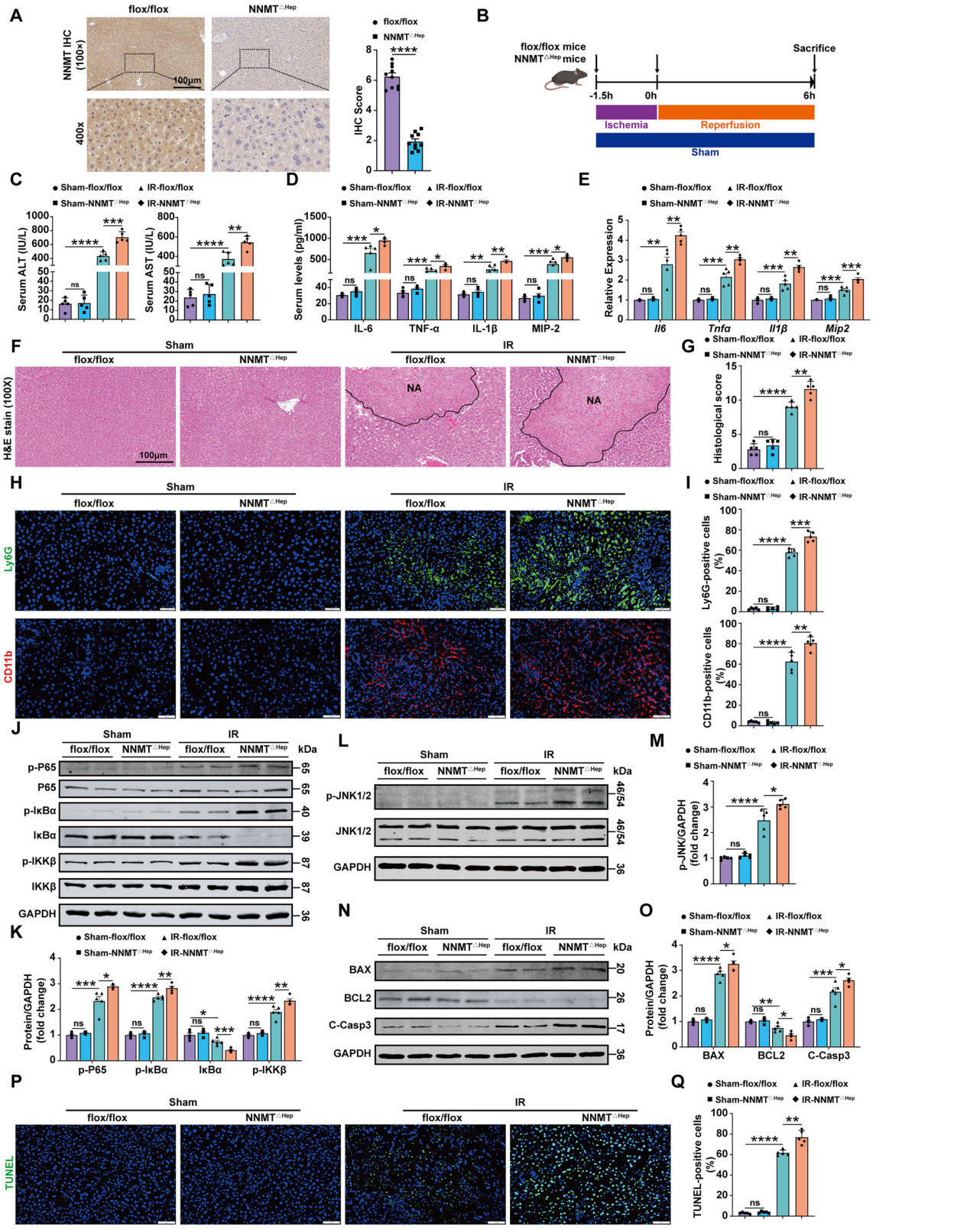

knockdown adenoviruses (Fig. S12D, E) and injected them into a mouse HIRI model (Fig. 6A). Our results showed that overexpression of ANGPT2 aggravated liver injury, inflammation, and apoptosis; conversely, knockdown of ANGPT2 had opposite effects in the context of HIRI (Figs. 6B–K and S13A–F). In vitro, ANGPT2 overexpression inhibited the viability of primary hepatocytes after H/R and increased levels of cell death and inflammation (Fig. S14A–C, G, H). Conversely, knockdown of ANGPT2 alleviated the viability of hepatocytes and inhibited cell death and inflammation (Fig. S14D–F, I, J). These results suggested that ANGPT2 could, in a cell-autonomous manner, worsen ischemia-reperfusion-induced cell death and inflammation in the liver.

Previous studies[17,23] have shown that ANGPT2, as a secreted protein, plays a role in the function of endothelial cells. Thus, we examined whether hepatic ANGPT2 may also trigger vascular endothelial injury

Fig. 4 | Hepatocyte-specific *Nnmt* knockout exacerbated liver injury, inflammation and apoptosis induced by ischemia-reperfusion. **A** Immunohistochemical staining of NNMT in the livers (scale bar: 100 μm) ($n = 10$, $P = 0.0000000002$). **B** Illustration of the experimental procedures. **C** The serum transaminase levels in mice ($n = 5$, $P = 0.0000004$, 0.00031, 0.000004, 0.003313). **D** The serum levels of inflammation cytokines in mice ($n = 5$, $P = 0.00296$, 0.0282, 0.000501, 0.032454, 0.001316, 0.00705, 0.00401, 0.04666). **E** The mRNA level of inflammation cytokines in the liver ($n = 5$, $P = 0.001061$, 0.06148, 0.000207 000193, 0.000544, 0.001082, 0.00187, 0.000905). **F**, **G** The extent of liver injury and necrosis following HIRI (scale bar: 100 μm) ($n = 5$, $P = 0.000001$, 0.002501). **H**, **I** The population of Ly6G- and CD11b-positive cells in the liver (scale bar: 50 μm) ($n = 5$, $P = 0.000000001$, 0.000471, 0.0000005, 0.006216). **J**, **K** The NF-κB signaling pathway in the liver ($n = 5$, $P = 0.00011$, 0.016125, 0.00000001, 0.00256, 0.025562, 0.000833, 0.000035, 0.008382). **L**, **M** The JNK signaling pathway in the liver ($n = 5$, $P = 0.000082$, 0.018456). **N**, **O** The apoptosis signaling pathway in the liver ($n = 5$, $P = 0.0000001$, 0.038022, 0.008149, 0.012967, 0.000133, 0.037869). **P**, **Q** The population of TUNEL-positive cells in the liver (scale bar: 50 μm) ($n = 5$, $P = 0.00000000005$, 0.001386). Data are presented as mean ± SD. Three biologically independent experiments. Source data are provided as a Source Data file. Figure 4B was created in BioRender. Bing, Y. (2025) https://BioRender.com/vesbjfg. ALT Alann amino transferase, AST Aspartate amino transferase, BAX BCL2 associated X protein, BCL2 B cell lymphoma 2, C-Casp3 Cleaved caspase-3, CD11b Integrin subunit alpha M, flox/flox the control group of NNMT$^{\Delta Hep}$ mouse, H&E Hematoxylin & eosin, IHC Immunohistochemistry, *Il1β*/IL-1β Interleukin 1beta, IR: Ischemia reperfusion, *Il6*/IL-6 Interleukin 6, LDH Lactate dehydrogenase, Ly6G Lymphocyte antigen 6 complex locus G, *Mip2*/MIP-2 Macrophage Inflammatory Protein 2, NNMT Nicotinamide N-methyltransferase, NNMT$^{\Delta Hep}$ hepatocyte-specific *Nnmt* knockout mouse, *Tnfα*/TNF-α Tumor necrosis factor α, TUNEL Terminal dUTP Nick-End Labeling.

during HIRI. Indeed, ANGPT2 overexpression increased the expression of vascular adhesion molecules in mice during HIRI (Fig. 6L, M). The vascular permeability assay showed that ANGPT2 overexpression increased vascular permeability during HIRI (Fig. 6N). The knockdown of ANGPT2 decreased the expression of vascular adhesion molecules and vascular permeability (Fig. S15A–C). In vitro, we observed more secreted ANGPT2 in the culture media of primary hepatocytes following H/R, and this secretion was reduced upon overexpression of *Nnmt* and pretreatment with 1-MNA (Figs. 6O and S16A). We then used these conditioned mediums of hepatocytes to treat endothelia cells (C166 cells) and found that the conditioned media from hepatocytes with *Nnmt* overexpression or 1-MNA pretreatment, compared to the conditioned medium from control hepatocytes, resulted in less inflammation, apoptosis, and the expression level of adhesion molecules in C166 cells (Fig. 6P–R). In contrast, the exact opposite effects were observed when we treated C166 cells with the conditioned media from hepatocyte with knocked down *Nnmt* (Fig. S16B).

The above results suggest that ANGPT2 may aggravate HIRI by exacerbating liver inflammation, apoptosis, and vascular injury.

NNMT/1-MNA protected against HIRI in an ANGPT2-dependent manner

Our aforementioned-results advocate a hypothesis that, during liver surgeries, the downregulation of NNMT/1-MNA promotes the expression of ANGPT2 and, by which, aggravates liver injury. To test this hypothesis, we investigated whether knockdown of ANGPT2 would alleviate the negative impacts induced by *Nnmt* depletion (Fig. 7A). Our results demonstrated that knockdown of ANGPT2 lowered the levels of liver injury, inflammation, and apoptosis in NNMT$^{\Delta Hep}$ mice to levels comparable to those in control mice in the context of HIRI (Figs. 7B–M and S17A). In line with our hypothesis, the NNMT$^{\Delta Hep}$ mice had a significantly higher expression levels of vascular adhesion molecules and vascular permeability than the control mice, which were reversed by knockdown of ANGPT2 (Fig. 7N–P).

Next, we investigated whether ANGPT2 would inhibit the protective functions of NNMT and 1-MNA (Figs. S18 and S19). Our results demonstrated that overexpression of ANGPT2 compromised the protection against liver injury, inflammation, and apoptosis by NNMT overexpression (Figs. S17B and S18B–M) or treatment with 1-MNA (Figs. S17C and S19B–M) in the context of HIRI. The protective effects of NNMT and 1-MNA on endothelial cells and vascular permeability in HIRI was counteracted by ANGPT2 overexpression (Figs. S18N–P and S19N–P). Finally, we tested our hypothesis in vitro (Fig. S20). In line with our in vivo data, overexpression of ANGPT2 abolished the protective effects of 1-MNA in primary hepatocytes (Fig. S20A, B). The opposite is also true, knockdown of ANGPT2 alleviated the negative impacts induced by NNMT inhibitor (Fig. S20C, D).

However, the precise mechanism through which NNMT/1-MNA inhibition of ANGPT2 contributes to ameliorating HIRI remains elusive. Prior research has demonstrated that ANGPT2 is capable of activating the JNK signaling pathway[24]. Our study demonstrates that NNMT/1-MNA suppresses JNK phosphorylation, leading to anti-inflammatory effects, whereas ANGPT2 promotes JNK phosphorylation, exacerbating HIRI. The inhibitory effects of NNMT/1-MNA on JNK signaling pathway is attenuated by overexpression of ANGPT2. Therefore, we hypothesize that NNMT/1-MNA/ANGPT2 may regulate HIRI via the JNK signaling pathway. To investigate our hypothesis, we utilize the JNK signaling pathway activator Anisomycin and the inhibitor SP600125 in vitro to elucidate the role of JNK in the regulation of HIRI by NNMT/1-MNA/ANGPT2. We found that the protective effects of NNMT/1-MNA were counteracted by activating the JNK signaling (Fig. S21A–J), while inhibiting the JNK signaling pathway alleviated the negative impacts induced by ANGPT2 overexpression (Fig. S22A–E).

Taken together, we concluded that NNMT/1-MNA can alleviate liver inflammation, apoptosis, and vascular injury in the context of HIRI by suppressing ANGPT2 expression. NNMT/1-MNA/ANGPT2 may regulate HIRI via the JNK signaling pathway. The general schematic diagram is shown in Fig. 8.

Discussion

In this study, we observed decreased expression of NNMT in the liver and a reduction in 1-MNA levels following HIRI. Overexpression of *Nnmt* or supplementation with 1-MNA ameliorated liver injury, inflammation, and apoptosis induced by ischemia-reperfusion. Conversely, knockout or knockdown of *Nnmt*, or treatment with an NNMT-specific inhibitor, exacerbated ischemia-reperfusion-induced liver injury. Furthermore, NNMT/1-MNA functions through modulation of the AKT/FOXO1/ANGPT2/JNK axis.

The effects of *Nnmt* and 1-MNA is under debate[7–9,25–28]. While overexpression of *Nnmt* in the liver or treatment with 1-MNA has been shown to decrease liver cholesterol and triglycerides in mice[8], liver-specific knockout of *Nnmt* protected mice from non-alcoholic steatohepatitis[9]. Additionally, Song et al. demonstrated that hepatic inhibition of NNMT alleviated alcohol-induced liver injury[25]. Conversely, Ding et al. reported that both global NNMT overexpression and 1-MNA treatment alleviates liver injury in alcohol-fed mice[26]. These findings highlight the complexity of NNMT's role in liver diseases, suggesting that higher levels of NNMT and 1-MNA may not simply translate to a uniformly beneficial or detrimental outcome in chronic liver conditions. To date, the impact of NNMT or 1-MNA on acute liver events remains unclear. HIRI, which often occurs within hours during hepatectomy, liver transplantation or hemorrhagic shock, can lead to acute liver injury and acute-on-chronic liver failure[27]. In this study, we demonstrate the beneficial effects of hepatic NNMT and 1-MNA in the context of HIRI, indicating a protective role for NNMT in acute liver injury. Consistently, 1-MNA has been reported to protect the liver from damage in Concanavalin A-induced acute liver injury models through a

https://doi.org/10.1038/s41467-025-59968-9

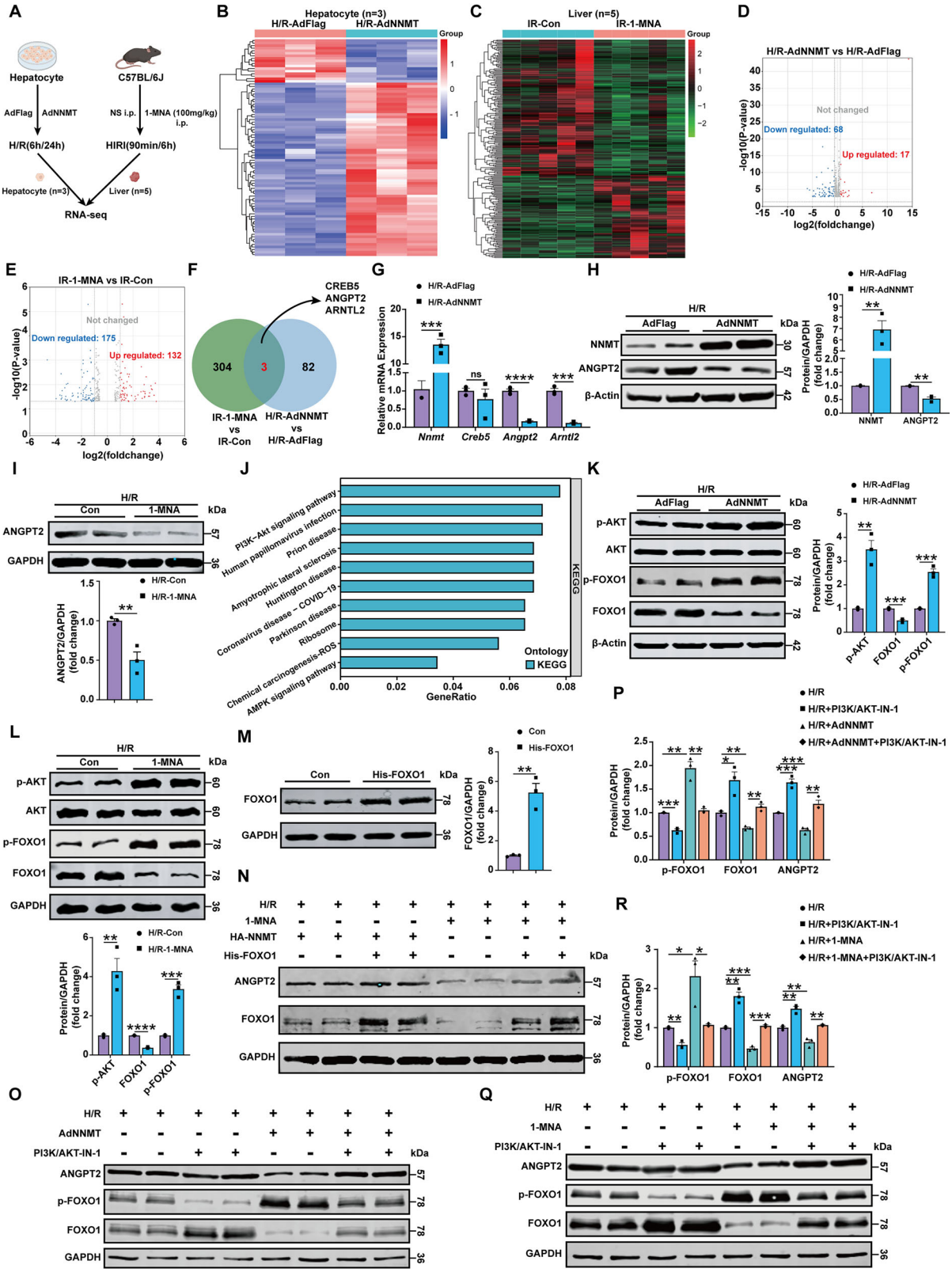

prostacyclin-dependent mechanism[7]. Specifically, 1-MNA inhibits the activation of the NLRP3 inflammasome in human liver macrophages, thereby attenuating the LPS-induced inflammatory response[28]. However, given the ongoing controversy surrounding NNMT's function in chronic liver disease, whether NNMT and 1-MNA exert similar or differing effects in other acute liver injury scenarios warrants future investigation.

In this study, we discovered that both the overexpression of *Nnmt* and pretreatment with 1-MNA inhibit ANGPT2 via the AKT/FOXO1 signaling pathway. While ANGPT2 has been extensively studied, its roles have primarily focused on vascular endothelial cells. Our investigation reveals that ischemia-reperfusion upregulates the expression and secretion of ANGPT2 in hepatocytes. Furthermore, hepatocyte-secreted ANGPT2 contributes to liver injury by directly

Fig. 5 | NNMT/1-MNA regulated the AKT/FOXO1/ANGPT2 axis. A RNA sequence of NNMT overexpressing hepatocytes under H/R stimulation, as well as in livers from C57BL/6J mice after 1-MNA pretreatment and subsequent HIRI. **B** Heatmap of cell transcriptome sequencing ($n = 3$). **C** Heatmap of tissue transcriptome sequencing ($n = 5$). **D** Cell transcriptome sequencing volcano map. **E** Tissue transcriptome sequencing volcano map. **F** Venn diagram of differentially expressed genes from both transcriptome sequencing. **G** Validation of the sequencing results by qRT–PCR in primary hepatocytes ($n = 3$, $P = 0.000255$, 0.466016, 0.000095, 0.000178). **H**, **I** The expression of NNMT and ANGPT2 in primary hepatocytes (**H**: $n = 3$, $P = 0.001665$; **I**: $n = 3$, $P = 0.008948$). **J** KEGG enrichment analysis of primary hepatocyte RNA sequencing. **K**, **L** The AKT/FOXO1 signaling pathway in primary hepatocytes (**K**: $n = 3$, $P = 0.007049$, 0.000026, 0.000449; **L**: $n = 3$, $P = 0.007049$, 0.000026, 0.000449). **M** Validation of the transfection efficiency of the FOXO1 overexpression plasmid ($n = 3$, $P = 0.002413$). **N** FOXO1 mediated the inhibition of ANGPT2 by NNMT/1-MNA during H/R in primary hepatocytes. **O**–**R** PI3K/AKT mediated the inhibition of ANGPT2 and FOXO1 by NNMT/1-MNA during H/R in primary hepatocytes (**P**: $n = 3$, $P = 0.002255$, 0.003152, 0.001284, 0.001528, 0.000862, 0.003306; **R**: $n = 3$, $P = 0.027408$, 0.032687, 0.00016, 0.000161, 0.008183, 0.003259). Data are presented as mean ± SD. Three biologically independent experiments. Source data are provided as a Source Data file. Figure 5A was created in BioRender. Bing, Y. (2025) https://BioRender.com/vesbjfg. AdFlag Gene overexpression negative control adenovirus, AdNNMT NNMT overexpression adenovirus, AKT Protein Kinase B, *Angpt2*/ANGPT2 Angiopoietin 2, *Arntl2* Basic helix-loop-helix ARNT like 2, *Creb5* cAMP responsive element binding protein 5, FOXO1 Forhead box O1, H/R Hypoxia and reoxygenation, IR Ischemia reperfusion, 1-MNA N^1-methylnicotinamide, *Nnmt*/NNMT Nicotinamide N-methyltransferase, PI3K/AKT-IN-1 A specific inhibitor of PI3K/AKT signaling pathway.

affecting hepatocytes and indirectly by inducing damage in endothelial cells. Thus, our findings offer additional insights into the biological function of ANGPT2 in the liver. However, the detailed mechanism underlying the crosstalk between hepatocytes and endothelia cells remains unclear. Based on existing literatures, several mechanisms may contribute. First, ANGPT2 overexpression disrupts endothelial homeostasis, leading to increased vascular permeability, the release of inflammatory mediators, and oxidative stress[17]. These changes impair hepatic blood supply and nutrient exchange, aggravating liver injury. Second, ANGPT2 activates inflammatory signaling pathways including NF-κB and Stat3[29], which promote the secretion of pro-inflammatory cytokines such as TNF-α and IL-6, thereby intensifying the hepatic inflammatory response. The release of these cytokines not only directly damages liver cells but also further impairs endothelial function, creating a vicious cycle. Moreover, ANGPT2 may influence hepatocyte proliferation and apoptosis by modulating cytokine secretion, such as TGF-β1[30]. In the context of the tumor microenvironment, inhibiting ANGPT2 expression or blocking its interaction with Tie2 has been shown to alleviate liver inflammation and fibrosis[31]. Specifically, in pancreatic neuroendocrine tumor hepatic metastasis, ANGPT2 inhibitors enhance T cell infiltration and activation, improving the tumor microenvironment. These findings highlight the critical role of ANGPT2 in mediating the interactions between hepatocytes and endothelial cells, thereby influencing hepatic pathophysiology through the regulation of vascular function, inflammatory responses, and immune evasion. Future research should explore precise mechanisms of ANGPT2's actions and develop therapeutic strategies targeting ANGPT2 to mitigate HIRI. Finally, a prior study suggests that FOXO1 may regulate ANGPT2 expression through binding to 5′ promoter region of ANGPT2[21], implying that the AKT/FOXO1 pathway could modulate ANGPT2 expression through direct interaction with the ANGPT2 promotor. However, further investigation is needed to clarify the specific mechanisms underlying this regulation and its relevance in the context of HIRI.

HIRI is a prevalent pathophysiological process encountered during liver resection and liver transplantation. Prolonged ischemia-reperfusion injury can lead to irreversible hepatic damage and, in severe cases, liver failure. Addressing how to alleviate HIRI and enhance the safety of liver resection and liver transplantation is an urgent and significant challenge that requires immediate attention. Currently, the treatment strategies for HIRI primarily include chemical intervention[32], ischemic preconditioning[13], and gene-targeted therapies[33]. However, there is still a lack of safe and effective clinical interventions to mitigate HIRI. Our study revealed that NNMT/1-MNA may protect HIIR via the AKT/FOXO1/ANGPT2/JNK pathway, potentially offering promising therapeutic targets and pharmacological strategies for the clinical prevention and treatment of HIRI. In addition, compared with the approach of constructing neutralizing antibodies to regulate ANGPT2 expression in the human body to reduce HIRI, 1-MNA, as a small-molecule compound and a safe food additive[34], may offer a more convenient alternative. Therefore, targeting NNMT and its enzymatic metabolite 1-MNA for the protection against HIRI may represent a more promising therapeutic target and pharmacological strategy, offering rapid clinical protection against HIRI.

Methods

Ethics approval

All animal experiments were approved by the Ethics Committee of the First Affiliated Hospital of Harbin Medical University. Written informed consent was obtained from all human participants. All procedures involving human samples were conducted in accordance with the guidelines approved by the Ethics Committee of the First Affiliated Hospital of Harbin Medical University.

Human liver tissue and serum

The human liver tissue and serum used in this study were obtained from patients undergoing partial hepatectomy for benign diseases. All patients and their family members willingly provided informed consent by signing the appropriate documentation, the clinical patient's information are listed in Supplemental Data 1. The initial liver tissue and serum samples (preoperative) were obtained prior to partial hepatectomy, while the second set of liver tissue and serum samples (postoperative) were collected before the conclusion of the surgical procedure. The utilization of clinical samples was conducted in accordance with the ethical approval granted by the Research Ethics Committee of the First Affiliated Hospital of Harbin Medical University. Western blot was employed to detect the expression of NNMT and ANGPT2 protein in clinical specimens, and serum 1-MNA levels were measured by reversed-phase high-performance liquid chromatography (HPLC).

Sex as a biological variable

For clinical human donor liver samples, both male and female subjects were examined. In animal models, estrogen has been demonstrated to play a role in regulating HIRI. To minimize variability associated with the female estrous cycle, only male mice were included in the study.

Cell culture

Mice were sequentially injected with calcium-free Hank's solution and Type IV collagenase solution via the portal vein for in situ live digestion. Subsequently the liver tissue was excised, minced, and incubated with Type IV collagenase solution for in vitro digestion. Following filtration through a 70 μm mesh and centrifugation at 50 g for 5 min, hepatocytes were successfully isolated. Mouse primary hepatocytes and mouse vascular endothelial C166 cell line were cultured in high glucose Dulbecco's modified Eagle's medium supplemented with 10% fetal bovine serum and 1%

https://doi.org/10.1038/s41467-025-59968-9

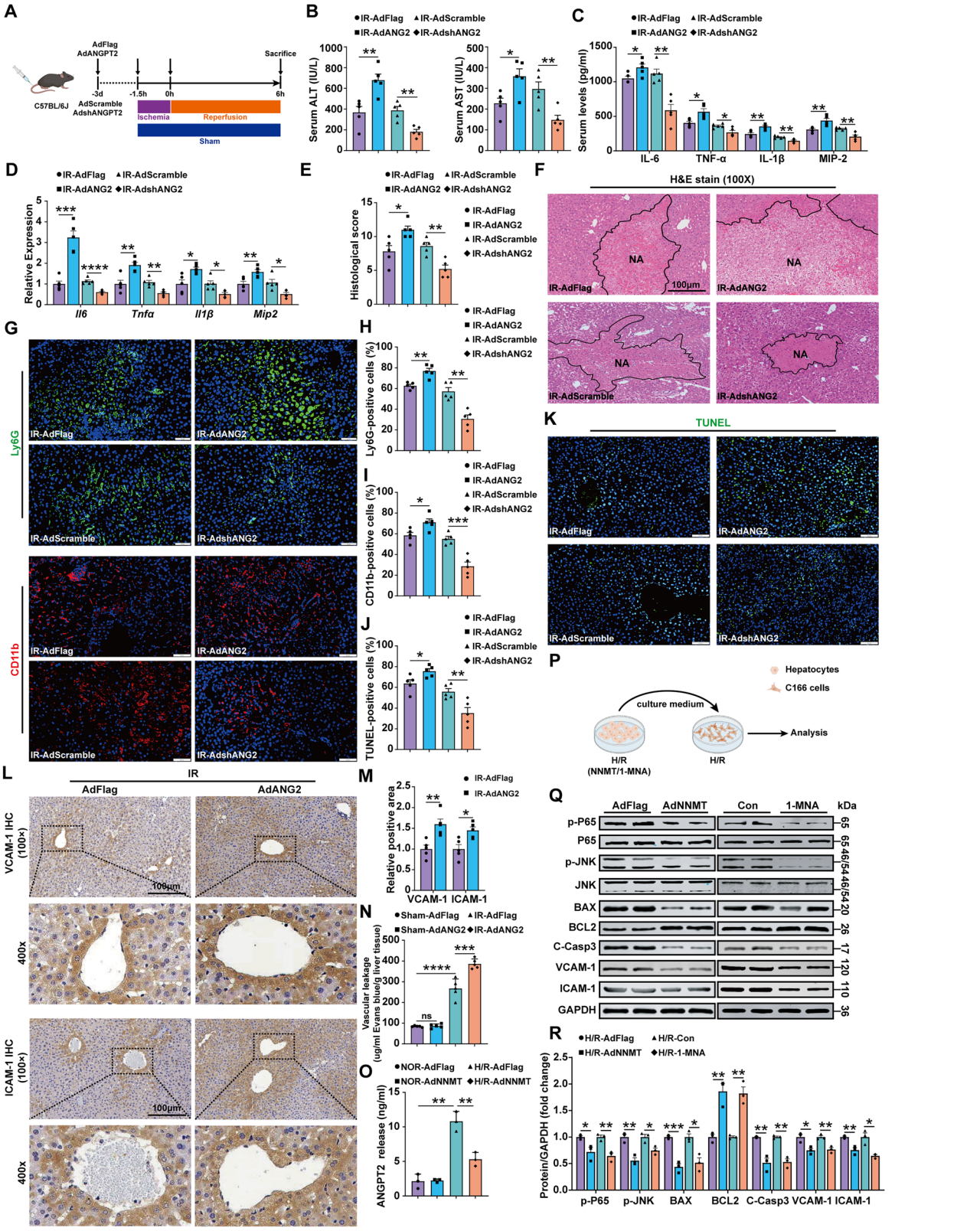

penicillin–streptomycin under a humidified atmosphere of 5% CO_2 at 37 °C.

Cell hypoxia/reoxygenation (H/R) model

The cells were cultured in an incubator (Biospherix, Lacona, NY, USA) under hypoxic conditions containing 1% O_2, 5% CO_2 and 94% N_2 at 37 °C for 6 h. Then, the cells were incubated under normoxic conditions with 95% air and 5% CO_2 for 6 h to obtain cell samples for subsequent qRT-PCR and Western blot analysis.

Animals

For the animal experiments, protocols followed standard procedures established by the Teaching and Research Committee for Using Living Animals, Harbin Medical University, China. C57BL/6 male mice,

Fig. 6 | ANGPT2 exacerbated HIRI-induced inflammation, apoptosis and vascular injury. A Illustration of the experimental procedures. **B**, **C** The levels of serum transaminase and inflammatory cytokines in these mice (**B**: $n = 5$, $P = 0.005305$, 0.001537, 0.142751, 0.006597; **C**: $n = 5$, $P = 0.028614$, 0.001121, 0.011263, 0.014709, 0.003263, 0.004605, 0.004984, 0.002186). **D** The mRNA level of inflammation cytokines in the liver ($n = 5$, $P = 0.000184$, 0.000087, 0.003713, 0.001586, 0.010984, 0.013157, 0.00887, 0.012965). **E**, **F** The extent of liver injury and necrosis (scale bar: 100 μm) ($n = 5$, $P = 0.01385$, 0.002319). **G**–**I** The population of Ly6G- and CD11b-positive cells in the liver (scale bar: 50 μm) (**H**: $n = 5$, $P = 0.001685$, 0.001053; **I**: $n = 5$, $P = 0.021513$, 0.000567). **J**, **K** The population of TUNEL-positive cells in the liver (scale bar: 50 μm) ($n = 5$, $P = 0.027668$, 0.00986). **L**, **M** Immunohistochemical staining of adhesion molecules in the livers (scale bar: 100 μm) ($n = 5$, $P = 0.00511$, 0.010282). **N** The vascular permeability in the liver ($n = 5$, $P = 0.000023$, 0.000907). **O** The secreted ANGPT2 in the culture media of primary hepatocytes ($n = 3$, $P = 0.001076$, 0.005631). **P** The C166 cells were treated with conditioned media obtained from hepatocytes pretreated with NNMT or 1-MNA during H/R. **Q**, **R** The NF-κB signaling pathway, JNK signaling pathway and apoptosis signaling pathway in the C166 cells treated with conditional media ($n = 3$, $P = 0.035456$, 0.005848, 0.00415, 0.021562, 0.00088, 0.012006, 0.00523, 0.002745, 0.00509, 0.001655, 0.017543, 0.006799, 0.007158, 0.011605). Data are showed as mean ± SD. Three biologically independent experiments. Source data are provided as a Source Data file. Figure 6A,P were created in BioRender. Bing, Y. (2025) https://BioRender.com/vesbjfg. AdANG2 ANGPT2 overexpression adenovirus, AdFlag Gene overexpression negative control adenovirus, AdScramble Gene knockdown negative control adenovirus, AdshANG2 ANGPT2 knockdown adenovirus, ALT Alann amino transferase, ANGPT2 Angiopoietin 2, AST Aspartate amino transferase, BAX BCL2 associated X protein, BCL2 B cell lymphoma 2, C-Casp3 Cleaved caspase-3, CD11b Integrin subunit alpha M, H&E Hematoxylin & eosin, H/R Hypoxia and reoxygenation, IHC Immunohistochemistry, IR Ischemia reperfusion, *Il1β*/IL-1β Interleukin 1 beta, *Il6*/IL-6 Interleukin 6, LDH Lactate dehydrogenase, Ly6G Lymphocyte antigen 6 complex locus G, *Mip2*/MIP-2 Macrophage Inflammatory Protein 2, 1-MNA N^1-methylnicotinamide, NNMT Nicotinamide N-methyltransferase, *Tnfα*/TNF-α Tumor necrosis factor α, TUNEL Terminal dUTP Nick-End Labeling.

including wild-type, non-transgenic (NTG), flox/flox, hepatocyte-specific *Nnmt* transgenic (NNMT-HTG) and hepatocyte-specific knockout of *Nnmt* ($NNMT^{\Delta Hep}$) mice were used in this study. The mice were randomly allocated into the experimental and control groups to ensure unbiased distribution. All animals were housed in a specific pathogen-free (SPF) animal laboratory at the Molecular Biology Centre of the Fourth Affiliated Hospital of Harbin Medical University under a 12-h light/dark cycle at 20–25 °C with 50–70% humidity, and free access to food and water. In our study, mice were euthanized via controlled carbon dioxide (CO_2) inhalation in accordance with established protocols for humane animal treatment. All animal experiments complied with the principles of the Animals in Research: Reporting In Vivo Experiments (ARRIVE) guidelines and incorporated the 3Rs principle (Replacement, Reduction, and Refinement).

Male C57BL/6 mice weighing 19–23 g and aged 6–8 weeks were purchased from Charles River Lab Animal Center (Beijing, China). Hepatocyte-specific *Nnmt* transgene mice (NNMT-HTG) were generated by Cyagen Bioscience using CRISPR/Cas9 technology. Non-transgenic (NTG) mice were utilized as littermate controls for NNMT-HTG mice. $NNMT^{\Delta Hep}$ mice with hepatocyte-specific knockout of *Nnmt* was kindly provided by professor Shangyu Hong[9]. Flox/flox mice were used as littermate controls for $NNMT^{\Delta Hep}$ mice.

Animal treatment

To establish the mouse HIRI mode, mice were anesthetized with 2% pentobarbital sodium (50 mg/kg), and a midline laparotomy was performed. Then, an atraumatic clip was clamped to the left lateral and median lobes of the liver to block 70% of the liver blood supply. At this time, it can be observed that the color of the surface of the target liver segment changes rapidly, so it is judged that the HIRI model is successfully constructed. After 90 min of ischemia, the clip was removed to allow for reperfusion. Liver tissue and serum were obtained at 0, 3, 6, 12, and 24 h after reperfusion. The sham group underwent an identical procedure without hepatic blood supply occlusion.

In the in vivo experiments, adenovirus vectors and control empty vectors (2×10^9 PFU per mouse) were intravenously injected via the tail vein 3 days prior to establishing the mouse HIRI model.

NNMT-specific inhibitor and 1-MNA

The NNMT-specific inhibitor (JBSNF-000088) and 1-MNA utilized in this study were procured from MedChemExpress Corporation (MCE, Shanghai, China). JBSNF-000088 was dissolved in cell culture medium at a concentration of 10 μM to establish the cell H/R model or injected into the mouse tail vein at a dose of 1 mg/kg and maintained for 4 h to induce the HIRI model. The cell H/R model was established by dissolving 1-MNA in the cell culture medium at a concentration of 10 mM. Alternatively, the HIRI model was constructed after 1-MNA was dissolved in normal saline at a ratio of 100 mg/kg and injected intraperitoneally for 1 h.

Other drugs treatment

The compound 10 μM PI3K/AKT-IN-1 (MCE, Shanghai, China) was utilized to inhibit the PI3K/AKT signaling pathway. 50 ng/ml of anisomycin (MCE, Shanghai, China) and 2 μmol/l of SP600125 (MCE, Shanghai, China) were used to activate and inhibit the JNK signaling pathway.

Adenovirus and plasmid construction and transfection

Adenovirus vectors for NNMT and ANGPT2 overexpression (AdNNMT; Ad-ANG2) and downregulation (AdshNNMT; AdshANG2) were constructed by GeneChem Corporation (Shanghai, China). The corresponding empty vectors (AdFlag; AdshNNMT) were used as negative controls (GeneChem, Shanghai, China). The sequence of the AdshNNMT adenovirus was 5′-GAGCAGTTTGAGGTGATTTCT-3′, while the sequence of the AdshANG2 adenovirus was 5′-GCUCGGUUGCUAUCCGUAATT UUACGGAUAGCAACCGAGCTT-3′. The overexpression plasmids of NNMT (HA-NNMT) and FOXO1 (His-FOXO1) were constructed and obtained from GeneChem Corporation (Shanghai, China). Primary hepatocytes were transfected with AdNNMT/AdFlag (MOI = 100), AdshNNMT/AdScramble (MOI = 100), Ad-ANG2/AdFlag (MOI = 100), or AdshANG2/AdScramble (MOI = 100) using sugar-free and serum-free DMEM. The HA-NNMT and His-FOXO1 plasmids were transfected into primary hepatocytes using Lipofectamine 2000 (Invitrogen, Carlsbad, CA). All adenoviruses were utilized in vitro following a minimum 72-h incubation period post cellular transfection.

Cell viability and apoptosis assay

Cell viability was assessed by a Cell Counting Kit-8 assay (CCK-8, Dojindo Molecular Technologies, CK04–13). A lactate dehydrogenase (LDH) assay kit from Promega (Madison, WI, USA) was utilized to quantify the LDH concentration in the culture medium for evaluating cell death. The optical density (OD) value was quantified using a microplate reader from Thermo Fisher Scientific (Madison, WI, USA).

Measurement of serum parameters

The concentration of 1-MNA was determined by reversed-phase high-performance liquid chromatography (HPLC). The experimental procedures for HPLC were performed as previously described[10]. The 1-MNA analytical standard was purchased from Sigma-Aldrich (St. Louis, MO, USA). The serum levels of alanine aminotransferase (ALT) and aspartate aminotransferase (AST) were measured by specific assay kits (Nanjing Jiancheng Bioengineering Institute, Nanjing, China). Serum inflammation and chemokines (IL-6, IL-1β, TNF-α, MIP-2) were

https://doi.org/10.1038/s41467-025-59968-9

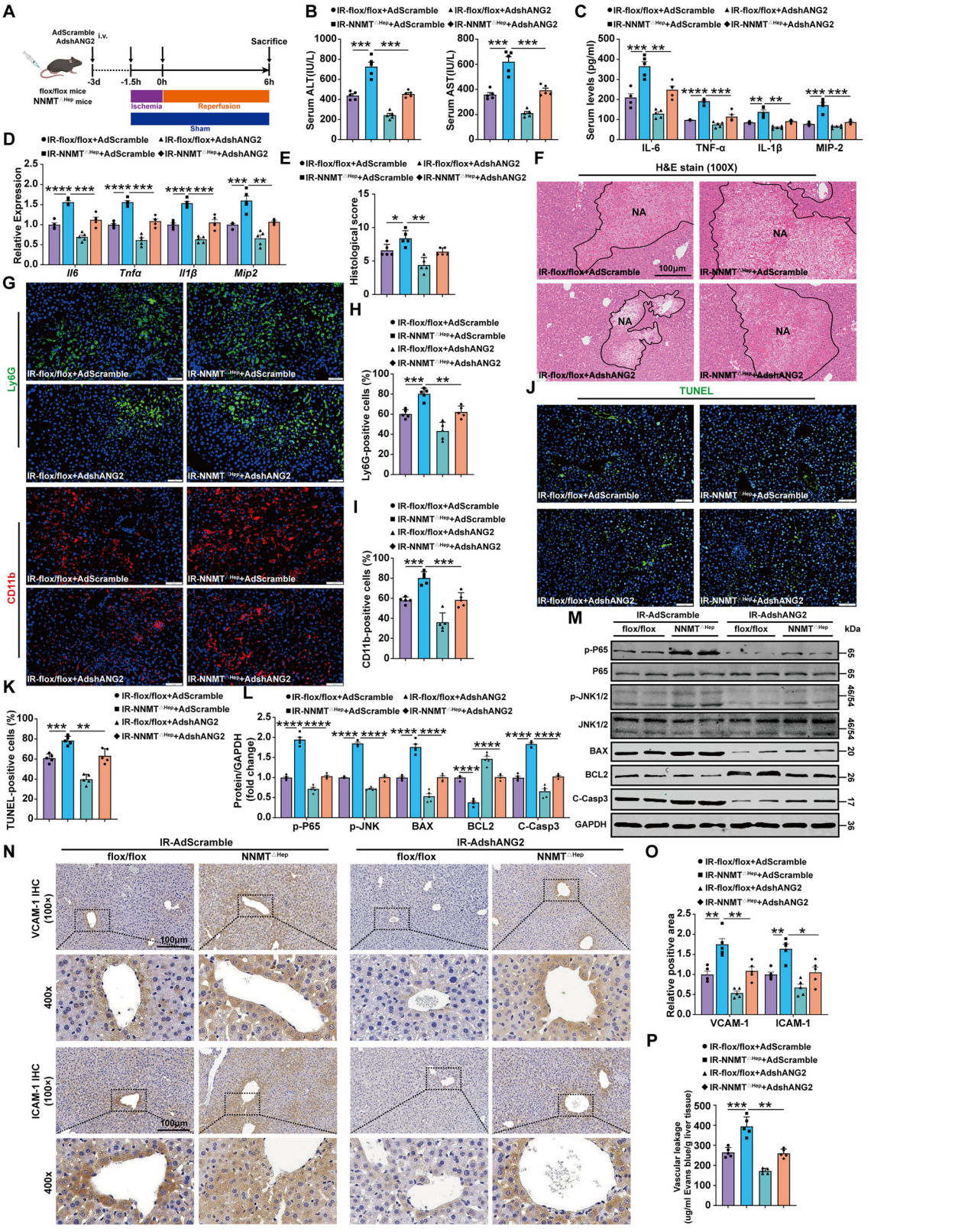

determined by enzyme-linked immunosorbent assay (ELISA) kits (R&D Systems, Minneapolis, MN). All procedures were conducted in accordance with the manufacturer's instructions.

Histological and immunofluorescence staining

Hematoxylin-eosin (H&E) staining was used to evaluate the extent of liver necrosis following HIRI. The liver tissues were fixed in 4% paraformaldehyde, followed by paraffin embedding and sectioning into 5 mm slices. After dewaxing, the sections were stained with hematoxylin and eosin and examined under an optical microscope (Olympus, Tokyo, Japan). Ly6G and CD11b immunofluorescence staining were employed to assess the extent of hepatic inflammatory infiltration. The liver tissue sections were photographed under a confocal laser scanning microscope

Fig. 7 | Knockdown of ANGPT2 alleviated the negative impacts induced by *Nnmt* depletion. A Illustration of the experimental procedures. **B**, **C** The levels of serum transaminase and inflammatory cytokines in these mice (**B**: $n = 5$, $P = 0.000329$, 0.000408, 0.000335, 0.000904; **C**: $n = 5$, $P = 0.000804$, 0.004003, 0.0000004, 0.000295, 0.001209, 0.00296, 0.000106, 0.000274). **D** The mRNA level of inflammation cytokines in the liver ($n = 5$, $P = 0.000007$, 0.000365, 0.000003, 0.000109, 0.000018, 0.000392, 0.00094, 0.001724). **E**, **F** The extent of liver injury and necrosis (scale bar: 100 μm) ($n = 5$, $P = 0.024019$, 0.00767). **G**, **I** The population of Ly6G- and CD11b-positive cells in the liver (scale bar: 50 μm) (**H**: $n = 5$, $P = 0.000249$, 0.00767; **I**: $n = 5$, $P = 0.000104$, 0.00767). **J**, **K** The population of TUNEL-positive cells in the liver (scale bar: 50 μm) ($n = 5$, $P = 0.000168$, 0.00767). **L**, **M** The NF-κB signaling pathway, JNK signaling pathway and apoptosis signaling pathway in the liver ($n = 5$, $P = 0.000001$, 0.000001, 0.000000008, 0.00000005, 0.000008, 0.000013, 0.0000005, 0.000001, 0.0000001, 0.00000007). **N**, **O** Immunohistochemical staining of adhesion molecules in the livers (scale bar: 100 μm) ($n = 5$, $P = 0.001681$, 0.004893, 0.001125, 0.010131). **P** The vascular permeability in the liver ($n = 5$, $P = 0.000653$, 0.00767). Data are showed as mean ± SD. Three biologically independent experiments. Source data are provided as a Source data file. Figure 7A was created in BioRender. Bing, Y. (2025) https://BioRender.com/vesbjfg. AdScramble Gene knockdown negative control adenovirus, AdshANG2 ANGPT2 knockdown adenovirus, ALT Alann amino transferase, ANGPT2 Angiopoietin 2, AST Aspartate amino transferase, BAX BCL2 associated X protein, BCL2 B cell lymphoma 2, C-Casp3 Cleaved caspase-3, CD11b Integrin subunit alpha M, flox/flox The control group of $NNMT^{\Delta Hep}$ mouse, H&E Hematoxylin & eosin, IHC Immunohistochemistry, IR Ischemia reperfusion, *Il1β*/IL-1β Interleukin 1 beta, *Il6*/IL-6 Interleukin 6, LDH Lactate dehydrogenase, Ly6G Lymphocyte antigen 6 complex locus G, *Mip2*/MIP-2 Macrophage Inflammatory Protein 2, $NNMT^{\Delta Hep}$ hepatocyte-specific *Nnmt* knockout mouse, NNMT Nicotinamide N-methyltransferase, *Tnfα*/TNF-α Tumor necrosis factor α, TUNEL Terminal dUTP Nick-End Labeling).

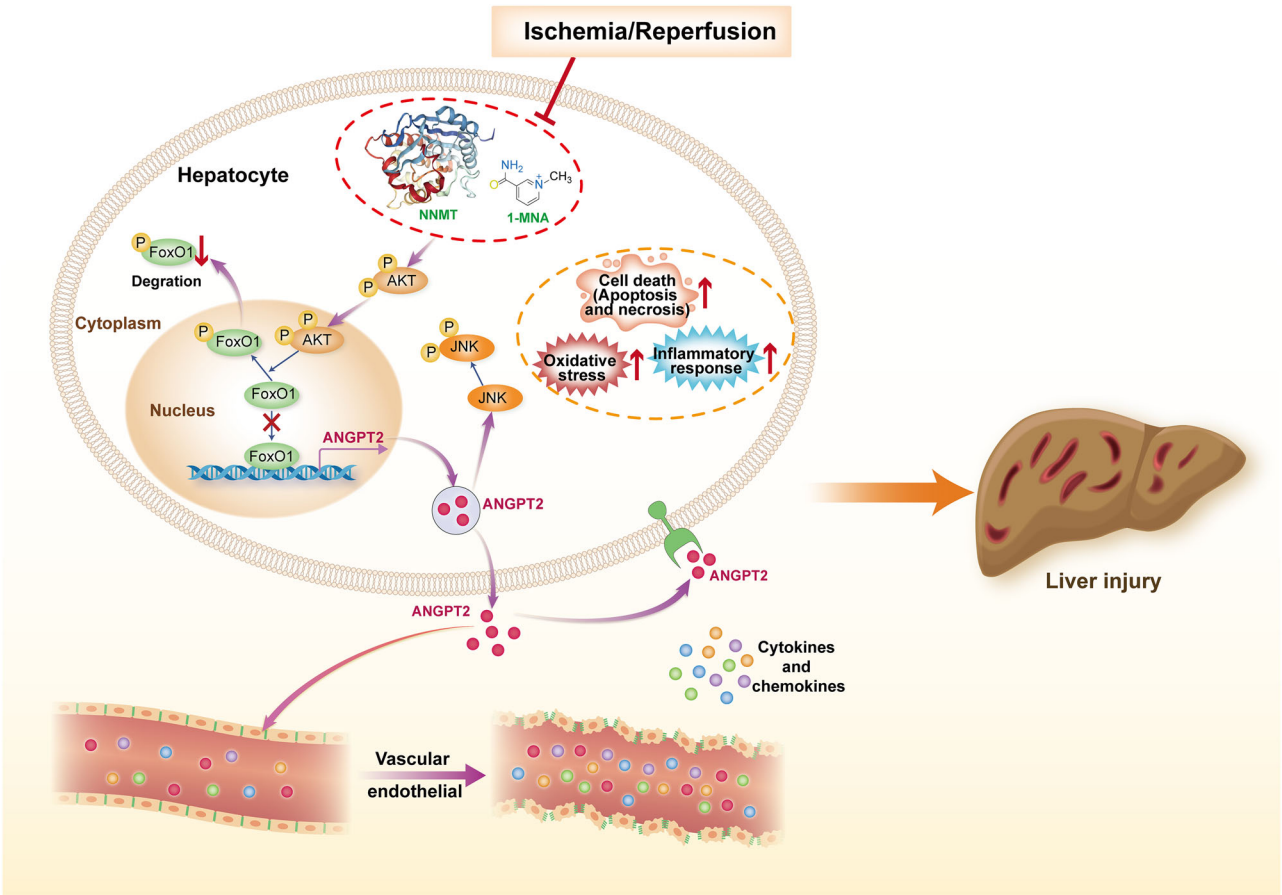

Fig. 8 | The general schematic diagram created with BioRender. Figure 8 was created using BioRender.com (https://BioRender.com/vesbjfg) and is released under a Creative Commons Attribution-NonCommercial-NoDerivs 4.0 International license (https://creativecommons.org/licenses/by-nc-nd/4.0/deed.en).

(Carl Zeiss, Germany) after incubation with primary antibodies against Ly6G (Cell Signaling Technology) (1:500) (88876) and CD11b (ABclonal) (1:200) (A1581) and fluorescently labeled secondary antibodies.

Terminal dUTP nick-end labeling (TUNEL) staining

A specific TUNEL kit (Roche, Shanghai, China) was utilized to evaluate the extent of apoptosis following HIRI according to the manufacturer's instructions. The TUNEL-positive cells were quantified under high magnification, and the percentage of TUNEL-positive cells was determined.

Immunohistochemistry (IHC)

The paraffin-embedded sections were sequentially processed for deparaffinization, rehydration, antigen retrieval using EDTA, and blocking with 10% bovine serum albumin (BSA) at 37 °C for 1 h. Subsequently, the sections were incubated with primary antibodies overnight at 4 °C. Following this, the sections were incubated with the corresponding secondary antibodies at 37 °C for 1 h. Finally, the images were captured and analyzed under a light microscope. The primary antibodies used in this experiment were as follows: anti-NNMT (Aviva System Biology) (1:200) (OAAN01939), anti-VCAM-1 (Abcam) (1:500) (ab134047), and anti-ICAM-1 (Proteintech) (1:500) (16174-1-AP).

Vascular permeability test

To assess hepatic vascular permeability, mice were administered an intraperitoneal injection of Evans blue solution (50 μg/g) diluted in PBS 30 min prior to the induction of the HIRI model. The mice underwent 90 min of liver ischemia followed by 6 h of reperfusion, after which precooled PBS was infused through the portal vein at a rate of 3 ml/min for 10 min to eliminate circulating blood Evans blue dye in the hepatic sinuses. The liver tissue was collected and immersed in formamide (1 ml/g), followed by incubation at room temperature for 48 h. Subsequently, the absorbance of the supernatant was measured at a wavelength of 620 nm. The concentration of Evans blue in the sample was determined by utilizing the standard curve of Evans blue.

Western blot

RIPA lysis buffer was employed to extract proteins from liver tissues and cells. The protein samples were resolved by SDS–polyacrylamide gel electrophoresis and subsequently transferred onto PVDF membranes (Merck Millipore Ltd., Germany). The membranes were blocked with 5% non-fat milk in PBST for 1 h at room temperature, followed by incubation with primary antibodies overnight at 4 °C. Subsequently, the membranes were incubated with IRDye 800CW secondary antibodies (LI-COR USA, Catalog No. 925-32210, diluted 1:10,000) for 1 h at room temperature. Protein visualization and quantification were performed using the Odyssey® Imaging System (LI-COR, USA). Information on the primary antibodies is provided in Supplemental Data 2.

Quantitative real-time PCR

According to the manufacturer's instructions, total RNA was extracted from cells and tissues using a total RNA preparation kit (Axygen, USA), and cDNA was synthesized using a reverse transcription kit (TOYOBO, Japan). qRT–PCR was performed using SYBR qPCR Mix (Roche, Switzerland) on a real-time PCR system (Applied Biosystems 7500HT Instrument, China). Glyceraldehyde-3-phosphate dehydrogenase (GAPDH) was used as an internal reference, and the $2^{-\Delta\Delta CT}$ method was utilized for quantitative analysis of target gene expression. The sequences of primers used in this study are listed in Supplemental Data 3.

RNA sequencing and analysis

Transcriptome sequencing was conducted on liver tissues of mice subjected to HIRI following 1-MNA pretreatment ($n = 5$), as well as on primary hepatocytes treated with H/R following NNMT overexpression ($n = 3$). TRIzol (Invitrogen, Carlsbad, CA, USA) was used to extract the total RNA from all samples. A NanoDrop and Agilent 2100 bioanalyzer (Thermo Fisher Scientific, MA, USA) were used to quantify the total RNA, and then Oligo (dT)-attached magnetic beads were used to purify mRNA. The mRNA library was generated according to the manufacturer's instructions and finally generated as single-end 50-base reads on the BGIseq500 platform (MGI Tech Co., Ltd., Shenzhen, China). SOAPnuke (version 1.5.2) was used to filter the sequencing data, and HISAT2 (version 2.0.4), Bowtie2 (version 2.2.5), RSEM (version 1.2.12), and Pheatmap (1.0.8) software were used to analyze the clean reads. The expression levels of differentially expressed genes were calculated using DESeq2 (version 1.4.5) software with the criteria of a fold change value of 1.5 and an adjusted p value of less than 0.05.

Statistical analysis

Statistical analysis was performed using GraphPad Prism 10.4 software. All data are expressed as the mean ± standard deviation (SD). Two-tailed Student's t test (for two groups) or one-way ANOVA (for multiple groups) was used to determine the significance of differences between groups. $P < 0.05$ indicated statistically significant differences. ns: no significance, $^{*}P < 0.05$, $^{**}P < 0.01$, $^{***}P < 0.001$, $^{****}P < 0.0001$.

Reporting summary

Further information on research design is available in the Nature Portfolio Reporting Summary linked to this article.

Data availability

The RNA-seq data generated in this study have deposited in the Genome Sequence Archive (GSA) under accession code CRA023059. All other data of this study are available within the article and its Supplementary files. Source data are provided with this paper.

References

1. Yang, W., Chen, J., Meng, Y., Chen, Z. & Yang, J. Novel targets for treating ischemia-reperfusion injury in the liver. *Int. J. Mol. Sci*. **19**, 1302 (2018).
2. Zhai, Y., Petrowsky, H., Hong, J. C., Busuttil, R. W. & Kupiec-Weglinski, J. W. Ischaemia-reperfusion injury in liver transplantation-from bench to bedside. *Nat. Rev. Gastroenterol. Hepatol*. **10**, 79–89 (2013).
3. Gao, F. et al. Targeting the hepatic microenvironment to improve ischemia/reperfusion injury: new insights into the immune and metabolic compartments. *Aging Dis*. **13**, 1196–1214 (2022).
4. Tang, S. P. et al. Reactive oxygen species induce fatty liver and ischemia-reperfusion injury by promoting inflammation and cell death. *Front. Immunol*. **13**, 870239 (2022).
5. Llacuna, L. et al. Reactive oxygen species mediate liver injury through parenchymal nuclear factor-kappaB inactivation in prolonged ischemia/reperfusion. *Am. J. Pathol*. **174**, 1776–1785 (2009).
6. Hong, S. et al. Nicotinamide N-methyltransferase regulates hepatic nutrient metabolism through Sirt1 protein stabilization. *Nat. Med*. **21**, 887–894 (2015).
7. Jakubowski, A. et al. 1-Methylnicotinamide protects against liver injury induced by concanavalin A via a prostacyclin-dependent mechanism: a possible involvement of IL-4 and TNF-α. *Int. Immunopharmacol*. **31**, 98–104 (2016).
8. Kraus, D. et al. Nicotinamide N-methyltransferase knockdown protects against diet-induced obesity. *Nature* **508**, 258–262 (2014).
9. Li, D., Yi, C., Huang, H., Li, J. & Hong, S. Hepatocyte-specific depletion of Nnmt protects mice from non-alcoholic steatohepatitis. *J. Hepatol*. **77**, 882–884 (2022).
10. Lu, S. et al. NNMT promotes the progression of intrahepatic cholangiocarcinoma by regulating aerobic glycolysis via the EGFR-STAT3 axis. *Oncogenesis* **11**, 39 (2022).
11. Pissios, P. Nicotinamide N-methyltransferase: more than a vitamin B3 clearance enzyme. *Trends Endocrinol. Metab*. **28**, 340–353 (2017).
12. Wang, C. et al. LncRNA Hnf4αos exacerbates liver ischemia/reperfusion injury in mice via Hnf4αos/Hnf4α duplex-mediated PGC1α suppression. *Redox Biol*. **57**, 102498 (2022).
13. Hua, Y. et al. Integrative analysis of the roles of lncRNAs and mRNAs in ischaemic preconditioning to alleviate liver ischaemia-reperfusion injury in mice. *Biochem. Biophys. Res. Commun*. **627**, 30–38 (2022).
14. Xu, Y. et al. Integrative analysis of the roles of lncRNAs and mRNAs in itaconate-mediated protection against liver ischemia-reperfusion injury in mice. *J. Inflamm. Res*. **14**, 4519–4536 (2021).
15. Fagiani, E. & Christofori, G. Angiopoietins in angiogenesis. *Cancer Lett*. **328**, 18–26 (2013).
16. Hu, S., Cao, S., Tong, Z. & Liu, J. FGF21 protects myocardial ischemia-reperfusion injury through reduction of miR-145-mediated autophagy. *Am. J. Transl. Res*. **10**, 3677–3688 (2018).
17. Lee, S. J. et al. Angiopoietin-2 exacerbates cardiac hypoxia and inflammation after myocardial infarction. *J. Clin. Invest*. **128**, 5018–5033 (2018).
18. Li, J. & Gao, S. HOXB5-activated ANGPT2 promotes the proliferation, migration, invasion and angiogenic effect of esophageal

cancer cells via activating ERK/AKT signaling pathway. *Exp. Ther. Med.* **24**, 585 (2022).
19. Yang, S. et al. Immunoregulation and clinical significance of neutrophils/NETs-ANGPT2 in tumor microenvironment of gastric cancer. *Front. Immunol.* **13**, 1010434 (2022).
20. Hernández-Bartolomé, Á et al. Intrahepatic angiopoietin-2 correlates with chronic hepatitis C progression and is induced in hepatitis C virus replicon systems. *Liver Int* **37**, 1148–1156 (2017).
21. Ghosh, C. C. et al. Drug repurposing screen identifies Foxo1-dependent angiopoietin-2 regulation in sepsis. *Crit. Care Med.* **43**, e230–e240 (2015).
22. Daly, C. et al. Angiopoietin-1 modulates endothelial cell function and gene expression via the transcription factor FKHR (FOXO1). *Genes Dev.* **18**, 1060–1071 (2004).
23. Eklund, L. & Olsen, B. R. Tie receptors and their angiopoietin ligands are context-dependent regulators of vascular remodeling. *Exp. Cell Res.* **312**, 630–641 (2006).
24. Hou, H. et al. Angiopoietin 2 stimulates trophoblast invasion via a mechanism associated with JNK signaling. *Mol. Hum. Reprod.* **27**, gaab014 (2021).
25. Song, Q. et al. ER stress-induced upregulation of NNMT contributes to alcohol-related fatty liver development. *J. Hepatol.* **73**, 783–793 (2020).
26. Ding, Q., Ma, Y., Lai, S., Dou, X. & Li, S. NNMT aggravates hepatic steatosis, but alleviates liver injury in alcoholic liver disease. *J. Hepatol.* **74**, 1248–1250 (2021).
27. Hirao, H., Nakamura, K. & Kupiec-Weglinski, J. W. Liver ischaemia-reperfusion injury: a new understanding of the role of innate immunity. *Nat. Rev. Gastroenterol. Hepatol.* **19**, 239–256 (2022).
28. Sidor, K., Jeznach, A., Hoser, G. & Skirecki, T. 1-Methylnicotinamide (1-MNA) inhibits the activation of the NLRP3 inflammasome in human macrophages. *Int. Immunopharmacol.* **121**, 110445 (2023).
29. Chen, Z. et al. Gastric tumour-derived ANGPT2 regulation by DARPP-32 promotes angiogenesis. *Gut* **65**, 925–934 (2016).
30. Chen, Y. et al. ANGPT2/CAV1 regulates albumin transcytosis of glomerular endothelial cells under high glucose exposure and is impaired by losartan. *Nefrologia***44**, 50–60 (2024).
31. Zhu, J. et al. MYBL1 induces transcriptional activation of ANGPT2 to promote tumor angiogenesis and confer sorafenib resistance in human hepatocellular carcinoma. *Cell Death Dis.* **13**, 727 (2022).
32. Uylaş, M. U., Şahin, A., Şahintürk, V. & Alataş, O.Ö. Quercetin dose affects the fate of hepatic ischemia and reperfusion injury in rats: an experimental research. *Int. J. Surg.* **53**, 117–121 (2018).
33. Yu, H. et al. GRINA alleviates hepatic ischemia–reperfusion injury-induced apoptosis and ER-phagy by enhancing HRD1-mediated ATF6 ubiquitination. *J. Hepatol*. https://doi.org/10.1016/j.jhep.2025.01.012 (2025). Epub ahead of print.
34. Turck, D. et al. Safety of 1-methylnicotinamide chloride (1-MNA) as a novel food pursuant to Regulation (EC) No 258/97. *Efsa J.* **15**, e05001 (2017).

Acknowledgements

This work was supported by National Key R&D Program of China (2021YFA0804801 and 2019YFA0802302 to S.H.), National Natural Science Foundation of China (82370643 to Y.M., 31971082 and 32271217 to S.H.), Natural Science Foundation of Heilongjiang Province of China (LC2018037 to Y.M.), Scientific Foundation of the First Affiliated Hospital of Harbin Medical University (HYD2020JQ0007 and 2019L01 to Y.M.). Thanks to professor Shangyu Hong for providing hepatocyte-specific knockout of *Nnmt* (NNMT$^{\Delta Hep}$) mice.

Author contributions

Conceptualization: B.Y., B.Q., H.Y., S.H., and Y.M.; Methodology: B.Y., B.Q., H.Y., S.K., Z.L., Y.H., S.L., C.W., S.G., Z.L., Y.Z., Z.M., X.L., Y.X., Z.F., M.B., Y.F., and W.T.; Surgical procedures: B.Y., B.Q., H.Y., and Y.M.; Visualization: BY., B.Q., H.Y., S.K., and M.L.; Funding acquisition: S.H. and Y.M.; Project administration: S.H. and Y.M.; Supervision: Y.M.; Writing—original draft: B.Y., B.Q., and H.Y.; Writing—review & editing: S.H. and Y.M. The order of authorship was determined by overall contributions and approved by all the authors.

Competing interests

The authors declare no competing interests.

Additional information

Supplementary information The online version contains supplementary material available at https://doi.org/10.1038/s41467-025-59968-9.

Correspondence and requests for materials should be addressed to Shangyu Hong or Yong Ma.

Peer review information *Nature Communications* thanks Sascha David who co-reviewed with Mattia Müller, and the other, anonymous, reviewer(s) for their contribution to the peer review of this work. A peer review file is available.